I···N Halogen bonding in 1:1 co-crystals formed between 1,4-diiodotetrafluorobenzene and the isomeric n-pyridinealdazines (n = 2, 3 and 4): Assessment of supramolecular association and influence upon solid-state photoluminescence properties†

Chien Ing Yeo,[a] Yee Seng Tan,[a] Huey Chong Kwong,[a] Vannajan Sanghiran Lee[b] and Edward R. T. Tiekink*[a]

a Research Centre for Crystalline Materials, School of Medical and Life Sciences, Sunway University, 47500 Bandar Sunway, Selangor Darul Ehsan, Malaysia

b Department of Chemistry, University of Malaya, 50603 Kuala Lumpur, Malaysia

E-mail: edwardt@sunway.edu.my (ERTT)

ELECTRONIC SUPPLEMENTARY MATERIAL

Table S1. Selected geometric parameters (Å, °) in cocrystals **2**–**4**

Parameter	**2**	**3**	**4**
I1···N1	2.927(3)	2.856(2)	2.811(3)
I2···N3	–	–	2.836(3)
C1–I1	2.092(3)	2.094(3)	2.100(3)
C4–I2	–	–	2.096(4)
C4–N1	1.336(4)	1.339(4)	–
C8–N1	1.344(4)	1.340(4)	–
C7–N1	–	–	1.336(5)
C11–N1	–	–	1.338(5)
C9–N2	1.283(5)	1.280(4)	–
C12–N2	–	–	1.278(5)
C13–N3	–	–	1.342(5)
C17–N3	–	–	1.342(5)
N2–N2^{i}	1.405(5)	1.408(5)	1.403(6)
N4–N4^{ii}	–	–	1.410(6)
C2–C1–I1	120.7(2)	122.6(2)	121.2(3)
C3–C1–I1	122.1(3)	121.0(2)	–
C6-C1-I1	–	–	121.8(2)
C3–C4–I2	–	–	121.0(3)
C5–C4–I2	–	–	120.7(3)
C4–N1–C8	117.0(3)	117.2(3)	–
C7–N1–C11	–	–	117.5(3)
C13–N3–C17	–	–	117.3(3)
C9–N2–N2^{i}	111.5(3)	111.5(3)	–
C12–N2–N2^{i}	–	–	111.7(4)
C18–N4–N4^{ii}	–	–	111.6(4)
Symmetry operations			
i	1-*x*, 1-*y*, 1-*z*	-1-*x*, -*y*, 1-*z*	-½-x, -½-y, ½-z

ii 1-*x*, 1-*y*, -*z*

Table S2. The percentage contributions of interatomic contacts to the Hirshfeld surfaces of overall **2**–**4**, individual **1** in **2**–**4** and **n**-PyAld in **2**–**4**

Contact	**2**	**1**	**2-PyAld**	**3**	**1**	**3-PyAld**	**4**	**1**	**N1-4-PyAld**	**N3-4-PyAld**
H···H	15.0	0.0	24.8	12.3	0.0	20.7	16.3	0.0	21.3	20.2
H···C/C···H	13.8	9.3	14.8	11.1	6.0	14.1	14.8	3.2	17.5	18.5
H···N/N···H	4.1	0.0	6.8	5.3	0.0	9.0	12.1	0.0	15.1	16.3
H···F/F···H	24.6	28.4	18.9	26.9	30.9	21.3	23.9	29.7	19.0	20.0
I···H/H···I	10.9	21.9	7.8	13.1	22.4	8.6	9.4	24.6	8.1	6.8
C···C	6.2	3.3	8.0	5.7	4.7	6.4	6.3	6.3	5.7	6.0
C···N/N···C	4.3	3.1	4.7	5.8	5.0	5.9	1.3	0.2	1.5	1.7
C···F/F···C	1.9	1.6	1.9	3.2	3.7	2.6	6.2	12.3	3.7	3.0
C···I/I···C	6.1	9.2	3.6	5.8	7.2	4.3	2.0	5.3	0.6	0.7
N···F/F···N	5.4	5.6	4.7	3.5	3.6	3.1	3.7	3.6	3.7	3.3
N···I/I···N	2.8	6.3	4.0	3.4	7.3	4.0	1.7	6.9	3.8	3.5
F···F	2.4	5.2	0.0	3.0	6.5	0.0	0.1	0.2	0.0	0.0
F···I/I···F	2.5	6.1	0.0	0.9	2.7	0.0	1.3	4.7	0.0	0.0
I···I	0.0	0.0	0.0	0.0	0.0	0.0	0.9	3.0	0.0	0.0

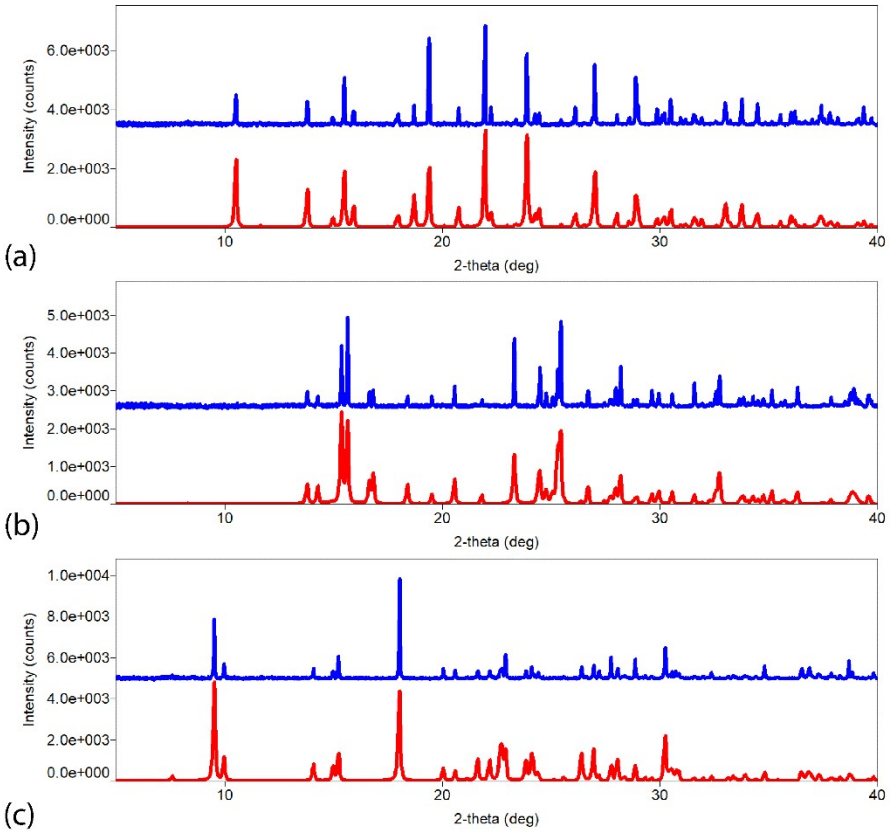

Figure S1. Experimental (blue trace) and simulated (red) powder X-ray diffraction patterns for (a) **2**, (b) **3** and (c) **4**, indicating matches between the single crystal results and structures of the bulk materials.

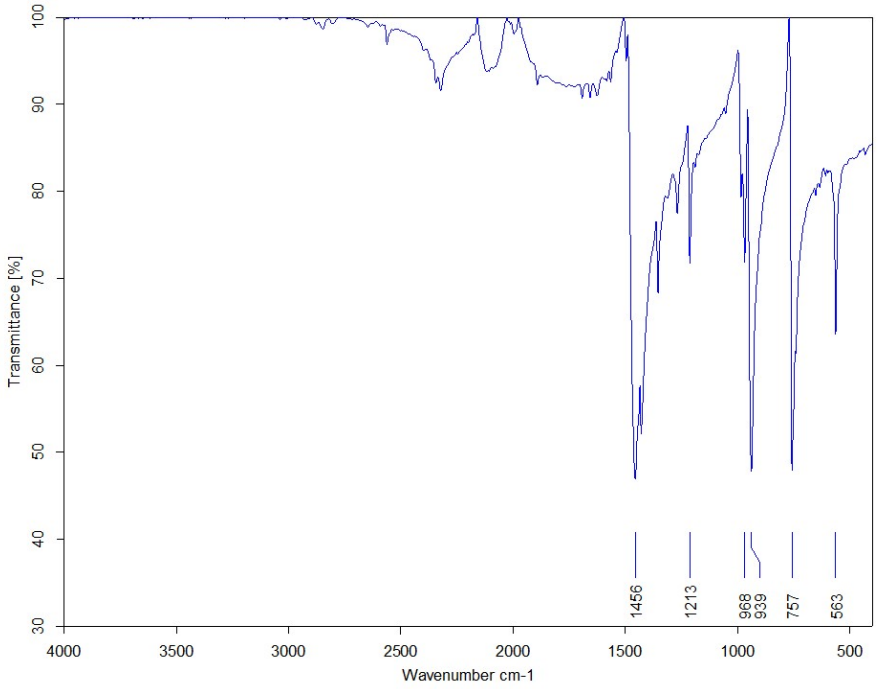
Transmittance [%]
Wavenumber cm-1
1456
1213
968
939
757
563

(a)

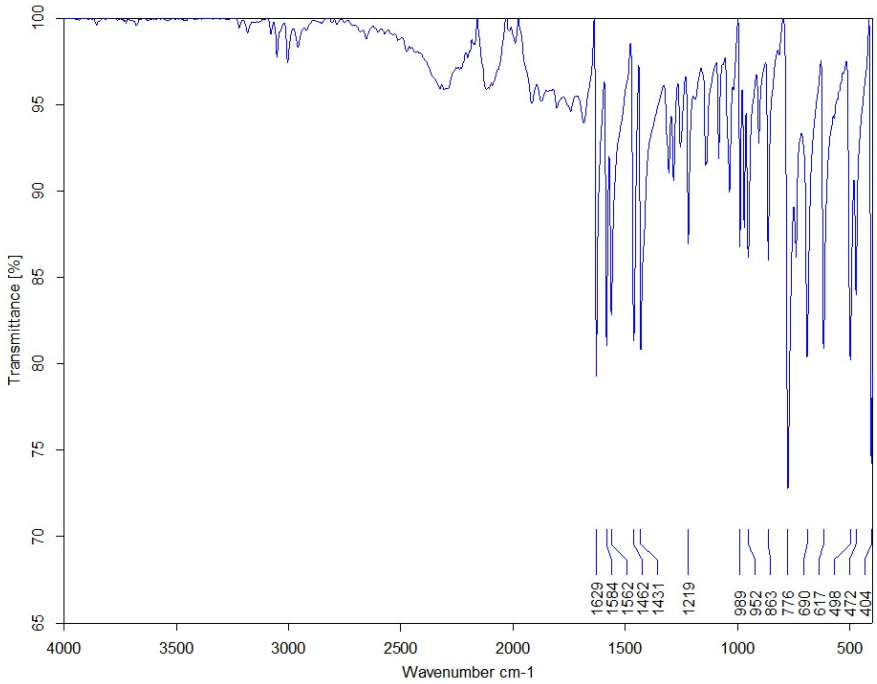
Transmittance [%]
Wavenumber cm-1
1629
1584
1562
1462
1431
1219
989
952
863
776
690
617
498
472
404

(b)

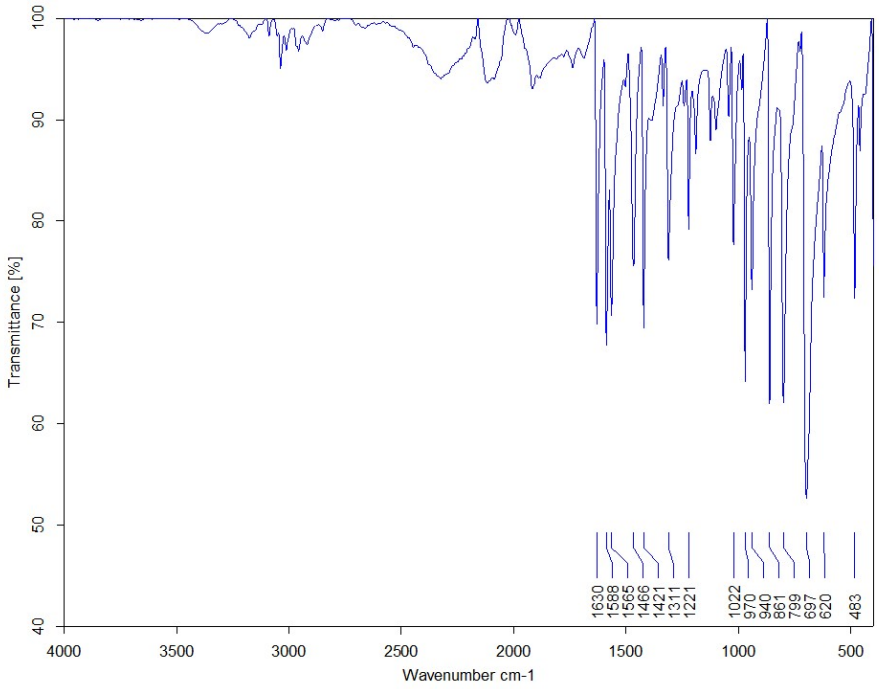
Transmittance [%]
Wavenumber cm-1
1630
1588
1565
1466
1421
1311
1221
1022
970
940
861
799
697
620
483

(c)

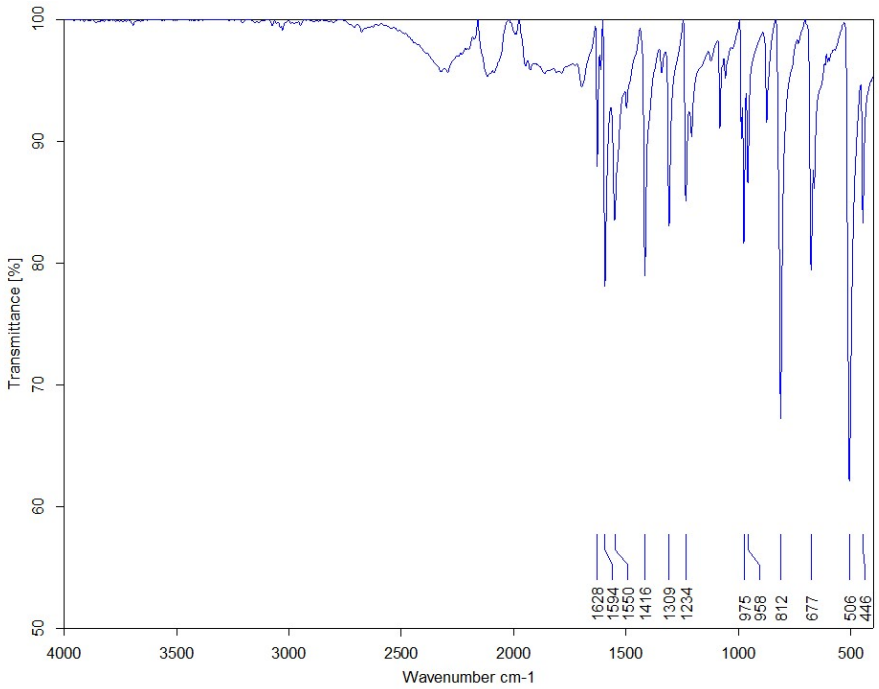
Transmittance [%]
Wavenumber cm-1
1628
1594
1550
1416
1309
1234
975
958
812
677
506
446

(d)

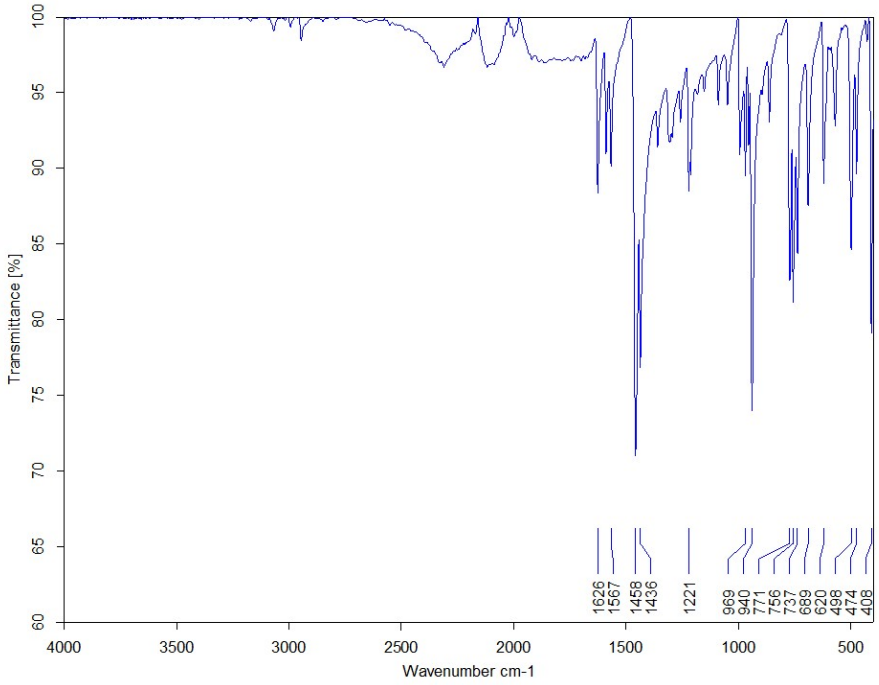
Transmittance [%]
100
95
90
85
80
75
70
65
60
4000
3500
3000
2500
2000
1500
1000
500
Wavenumber cm-1
1626
1567
1458
1436
1221
969
940
771
756
737
689
620
498
474
408

(e)

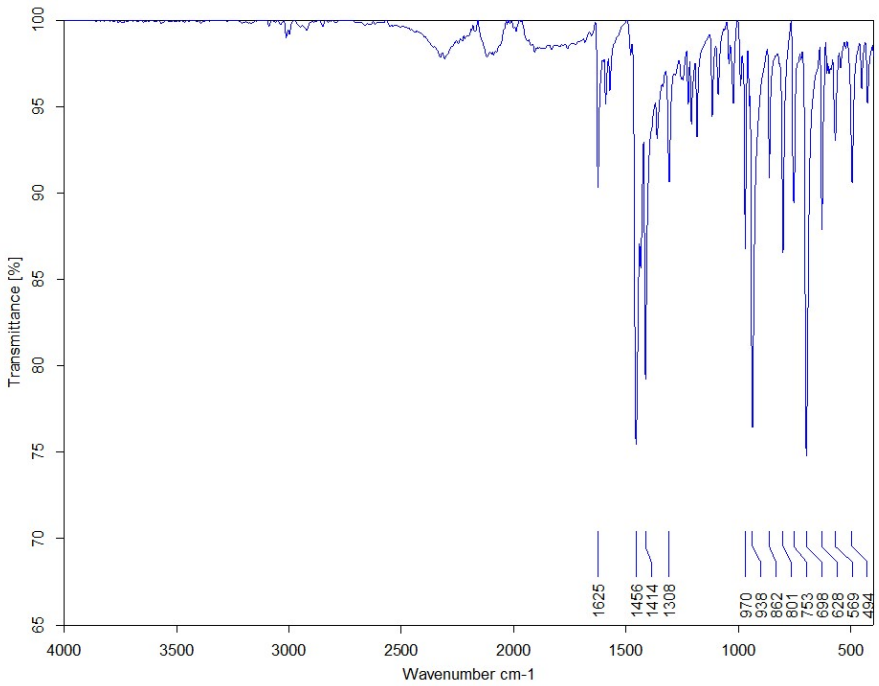
Transmittance [%]
100
95
90
85
80
75
70
65
4000
3500
3000
2500
2000
1500
1000
500
Wavenumber cm-1
1625
1456
1414
1308
970
938
862
801
753
698
628
569
494

(f)

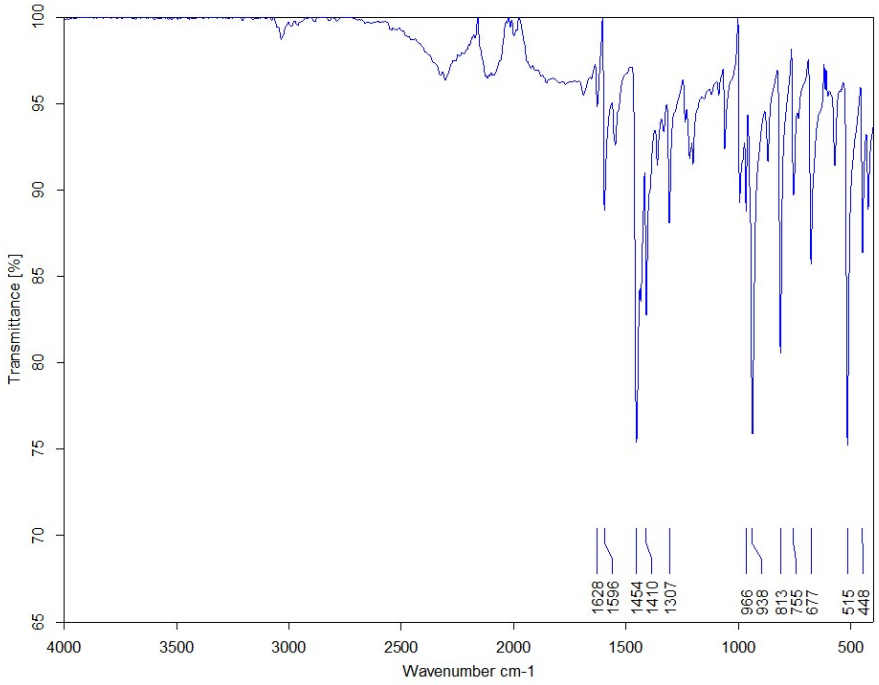

(g)

Figure S2. FTIR spectra for (a) **1**, (b) **2**-PyAld, (c) **3**-PyAld, (d) **4**-PyAld, (e) **2**, (f) **3** and (g) **4**.

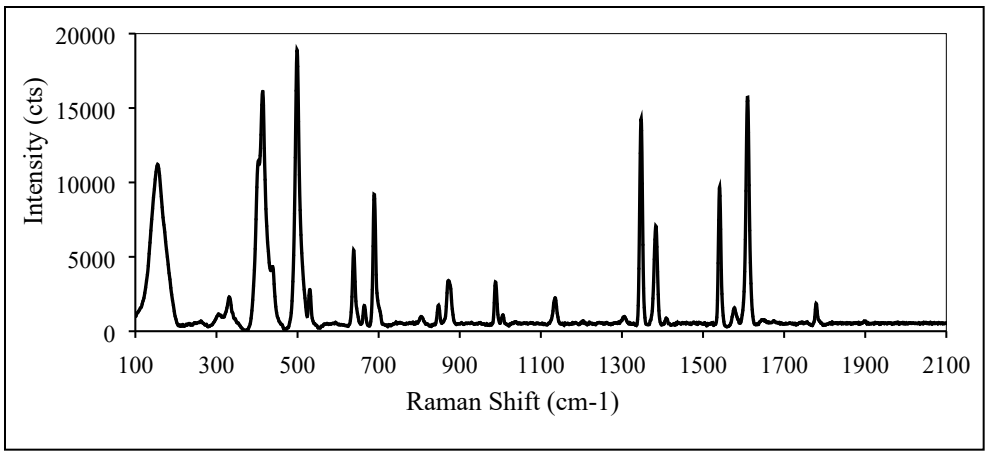
Intensity (cts)
20000
15000
10000
5000
0
100
300
500
700
900
1100
1300
1500
1700
1900
2100
Raman Shift (cm-1)

(a)

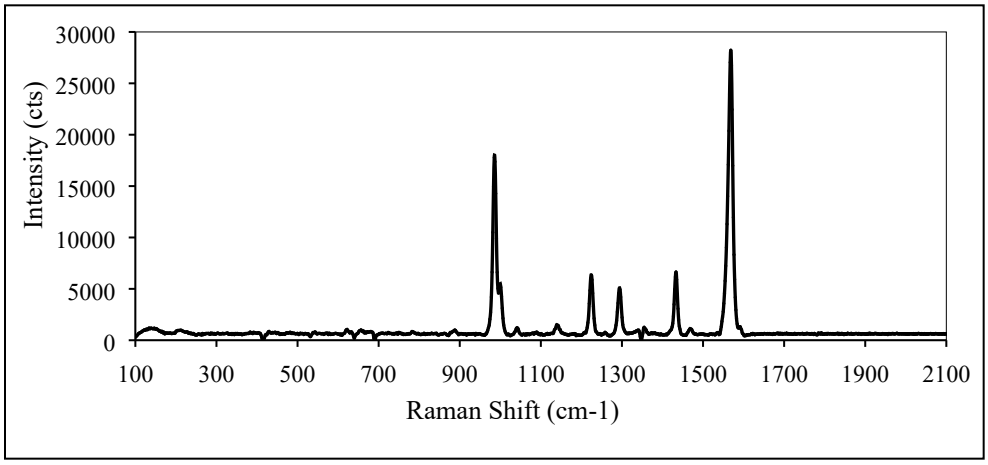
Intensity (cts)
30000
25000
20000
15000
10000
5000
0
100
300
500
700
900
1100
1300
1500
1700
1900
2100
Raman Shift (cm-1)

(b)

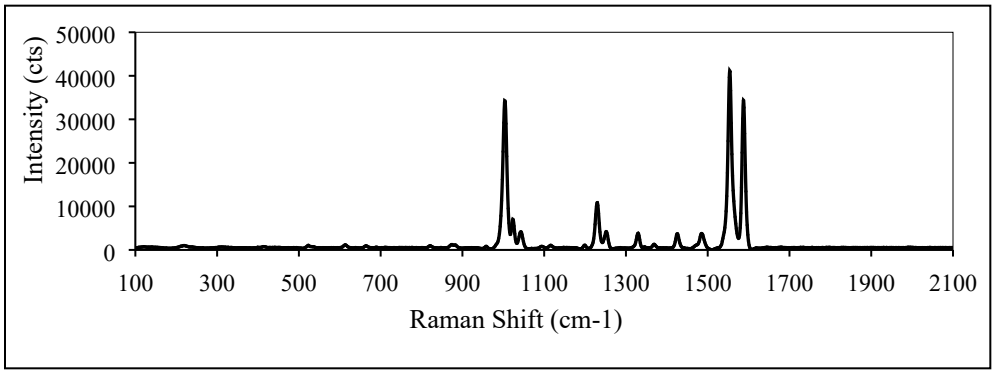
Intensity (cts)
50000
40000
30000
20000
10000
0
100
300
500
700
900
1100
1300
1500
1700
1900
2100
Raman Shift (cm-1)

(c)

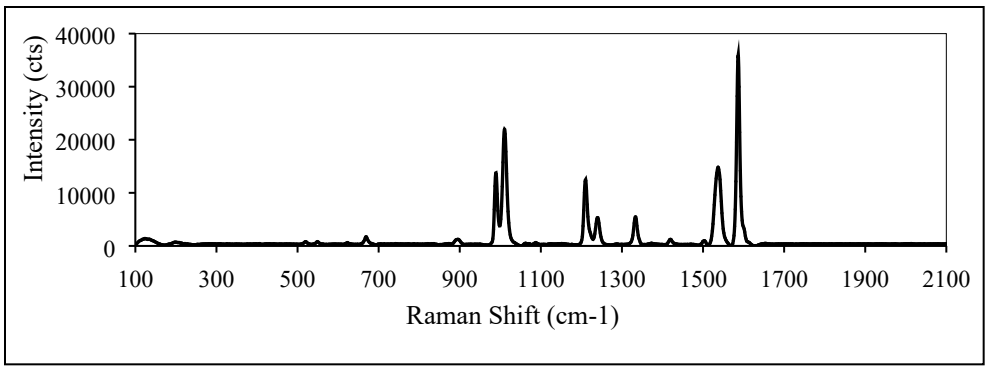
Intensity (cts)
40000
30000
20000
10000
0
100
300
500
700
900
1100
1300
1500
1700
1900
2100
Raman Shift (cm-1)

(d)

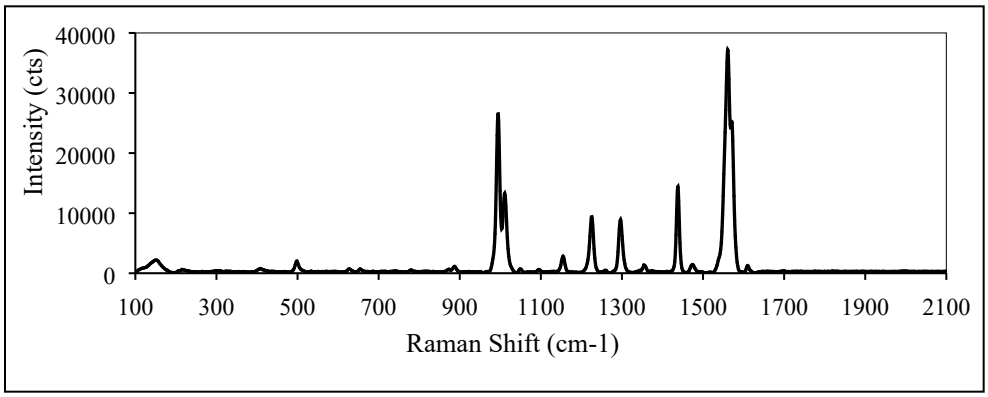
Intensity (cts)
40000
30000
20000
10000
0
100
300
500
700
900
1100
1300
1500
1700
1900
2100
Raman Shift (cm-1)

(e)

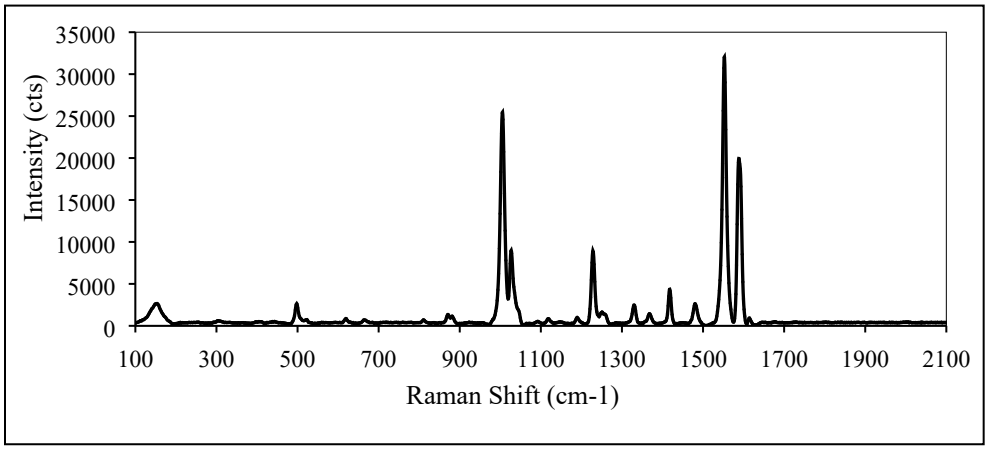
Intensity (cts)
35000
30000
25000
20000
15000
10000
5000
0
100
300
500
700
900
1100
1300
1500
1700
1900
2100
Raman Shift (cm-1)

(f)

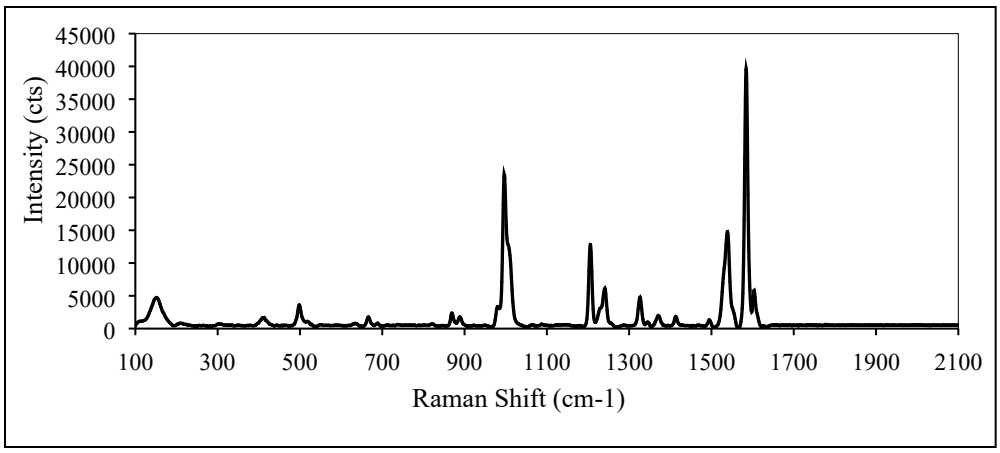

(g)

Figure S3. Raman spectra for (a) **1**, (b) **2**-PyAld, (c) **3**-PyAld, (d) **4**-PyAld, (e) **2**, (f) **3** and (g) **4**.

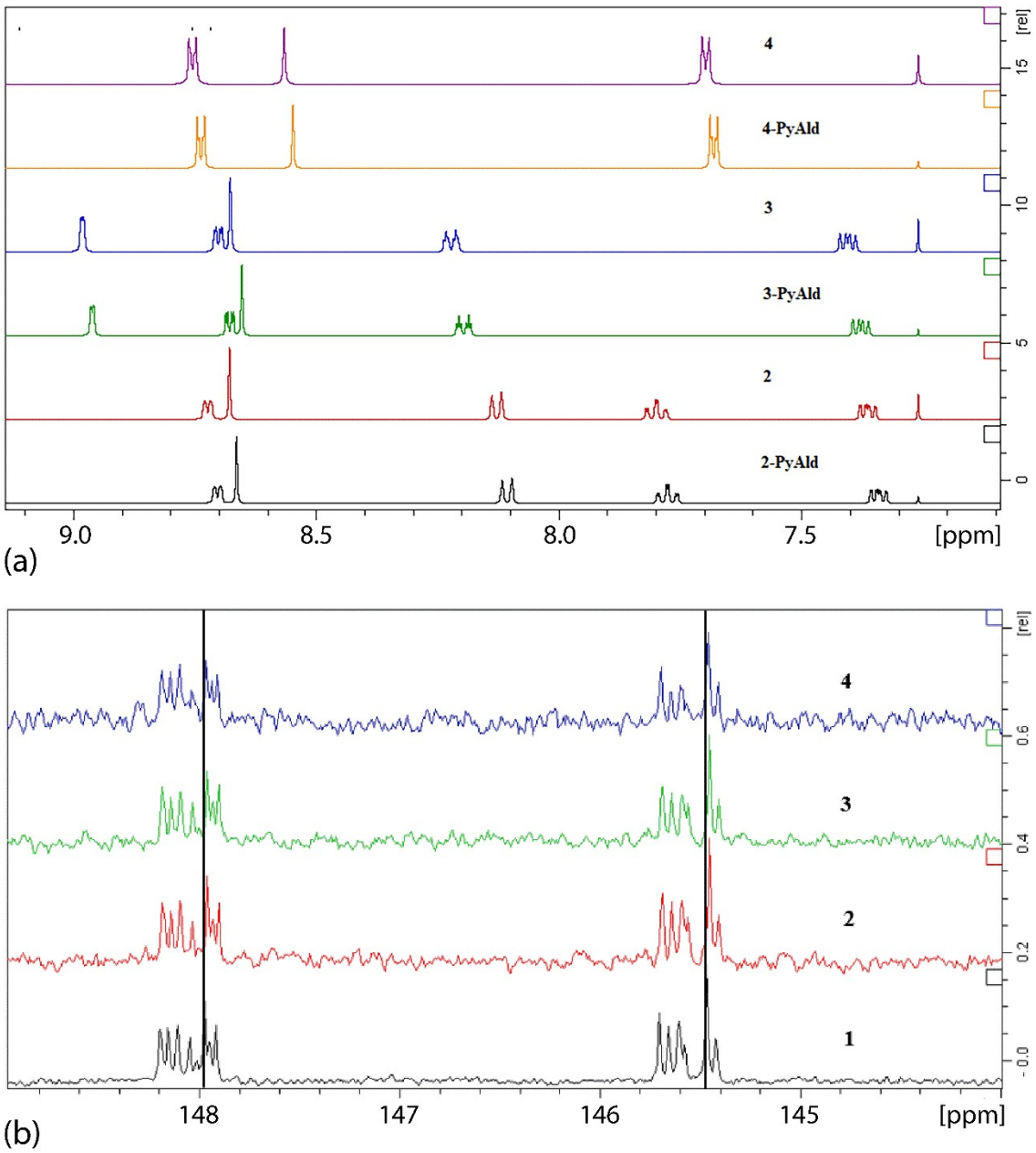

Figure S4. (a) ^{1}H NMR spectra for **2**–**4** and **n**-PyAld (**n** = 2, 3 and 4) and (b) ^{13}C{^{1}H} NMR spectra for **1**–**4**, recorded in 0.1 M $CDCl_3$ solution. Downfield shifts are noted for the characteristic resonances ascribed to **n**-PyAld. Upfield shifts of approximately 0.02 ppm were noted for the ^{13}C signals of **2**–**4** *cf*. **1** but no significant changes are observed for the ^{13}C resonances due to the **n**-PyAld molecules.

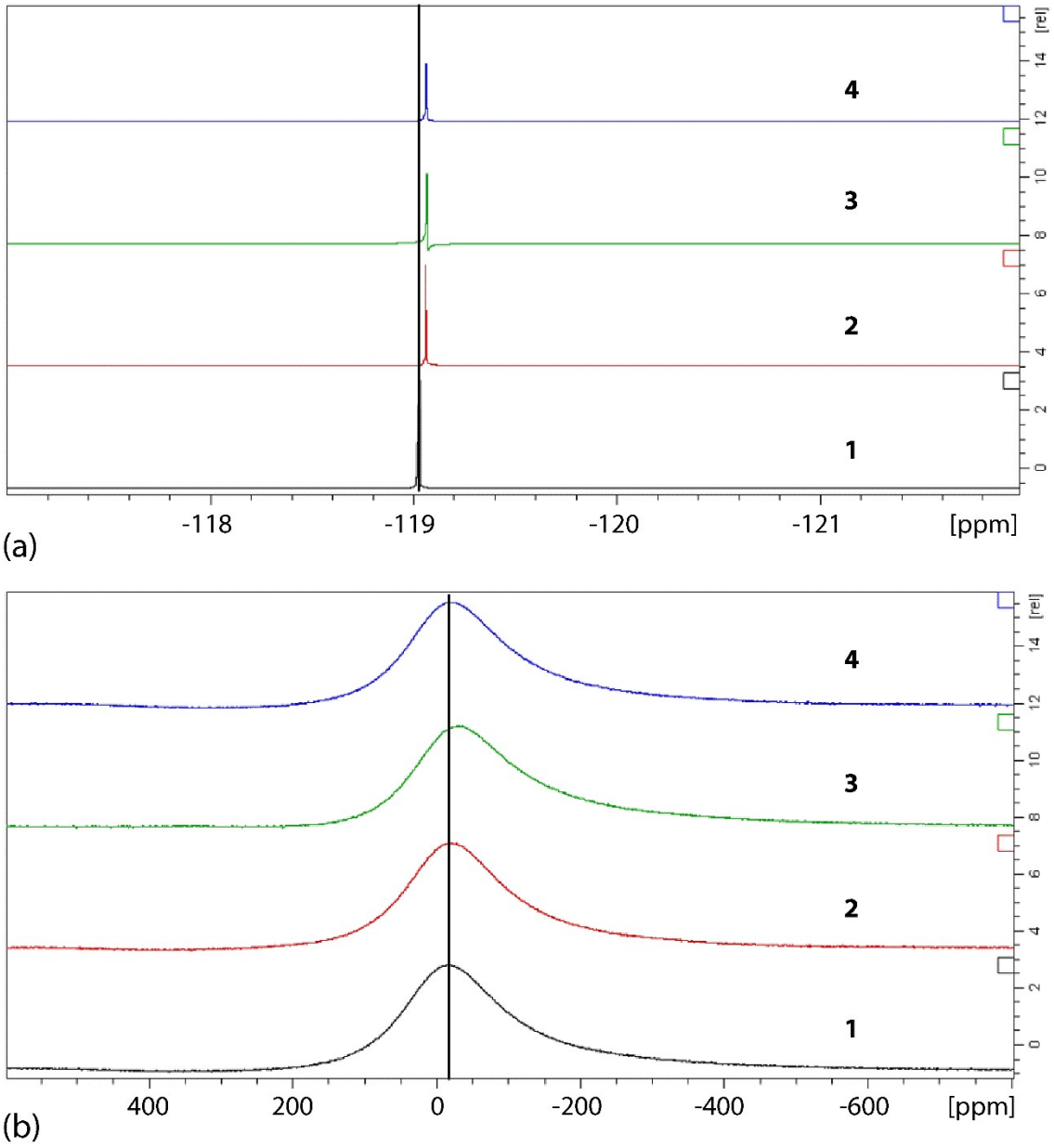

Figure S5. (a) ^{19}F and (b) ^{127}I NMR spectra recorded in 0.1 M $CDCl_3$ solution for **1**–**4**. Upfield shifts were observed for the ^{19}F and ^{127}I signals of coformer **1** in **2**–**4**, respectively.

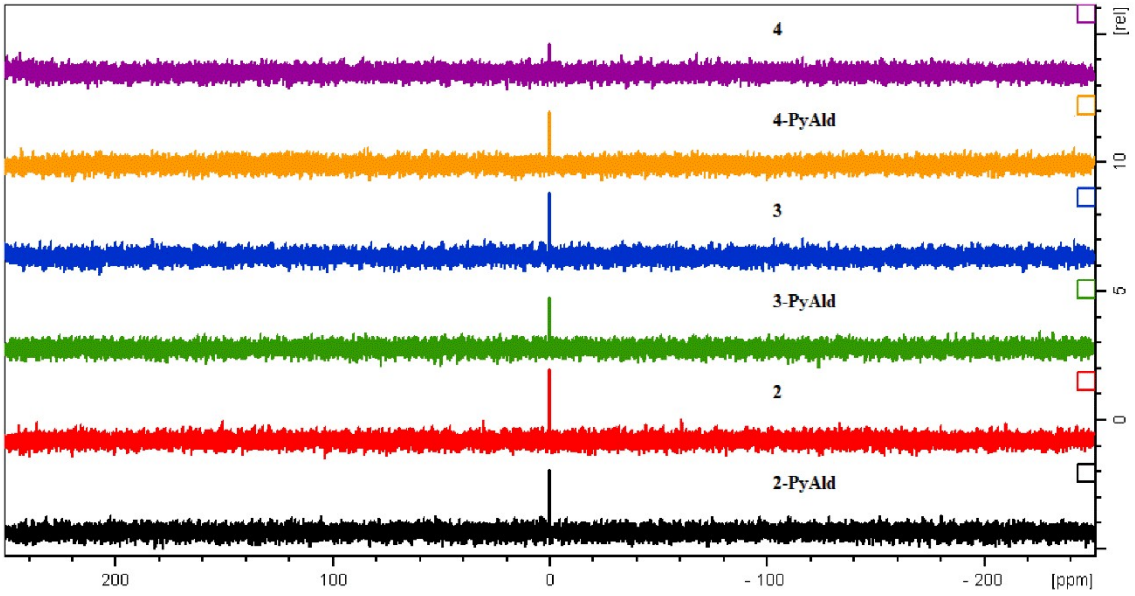

Figure S6. ^{15}N NMR spectra for **2**–**4** and **n**-PyAld (**n** = 2, 3 and 4) recorded in 0.1 M $CDCl_3$ solution. There are no visible changes observed in the ^{15}N NMR spectra of **2**–**4** in comparison to the respective **n**-PyAld coformers.

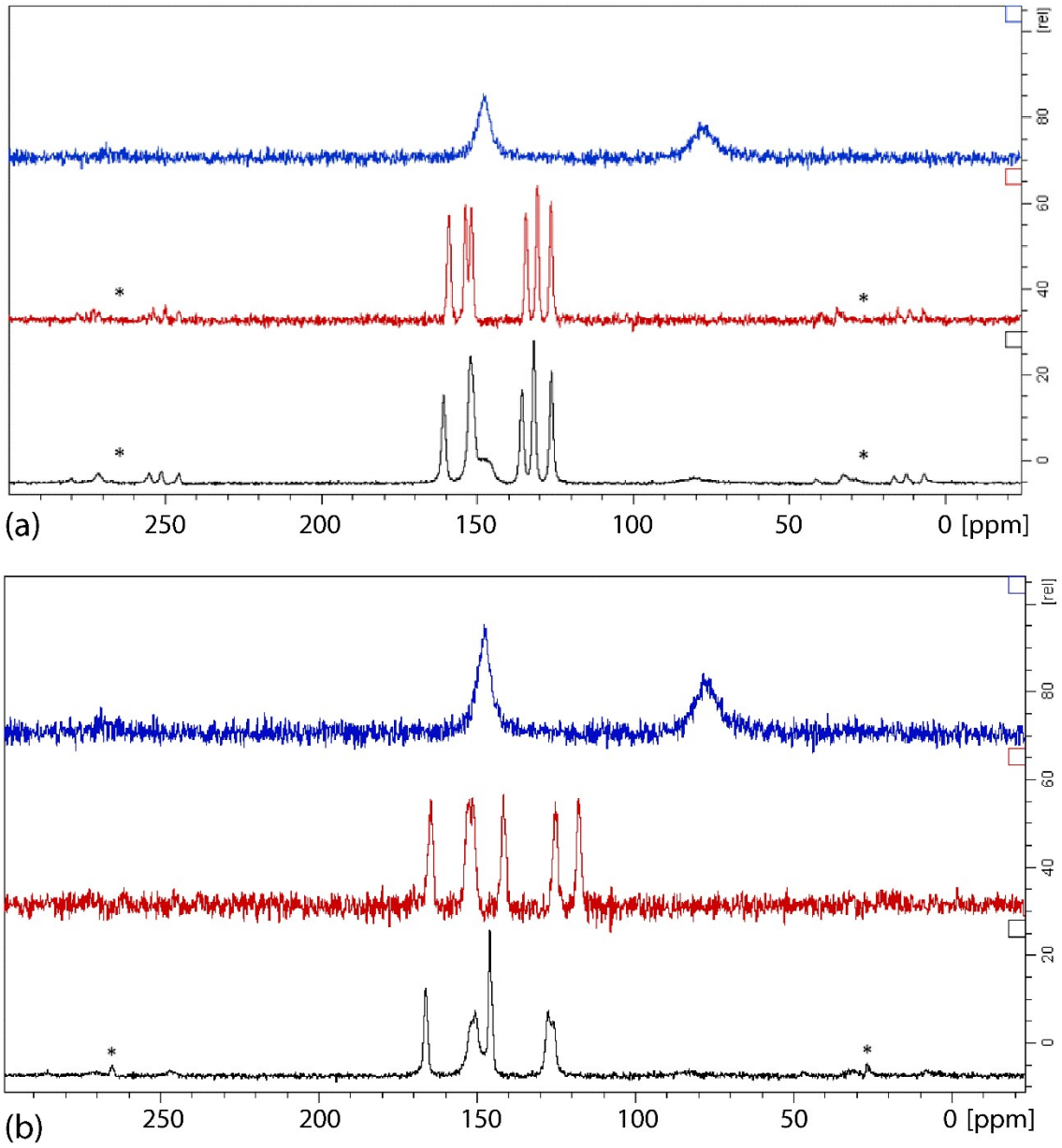

Figure S7. (a) $^{13}C\{^{1}H\}$ SS NMR spectra of **1** (blue trace), **3**-PyAld (red) and **3** (black) measured at 12 kHz, and (b) $^{13}C\{^{1}H\}$ SS NMR spectra for **1** (blue trace), **4**-PyAld (red) and **4** (black). Asterisks denote MAS spinning sidebands.